Proceedings of the Third International Conference on Intelligent Communication Technologies and Virtual Mobile Networks (ICICV 2021).
IEEE Xplore Part Number: CFP21ONG-ART; 978-0-7381-1183-4

2021 Third International Conference on Intelligent Communication Technologies and Virtual Mobile Networks (ICICV) | 978-1-6654-1960-4/20/$31.00 ©2021 IEEE | DOI: 10.1109/ICICV50876.2021.9388632

Screening Thyroid Tumor in Ultrasound Thyroid Images using Hidden Markov Model

B. Shankarlal
Department of ECE
Perunthalaivar Kamarajar Institute of Engg. & Tech., Karaikal, Puducherry, India
shankarlal.pkiet@gmail.com

P. D. Sathya
Department of ECE
Annamalai University, FEAT
Chidambaram, Tamilnadu, India
pd.sathya@yahoo.in

V. P. Sakthivel
Department of EEE
Govt. College of Engineering,
Dharmapuri, Tamilnadu, India
vp.sakthivel@gmail.com

***Abstract*—Detection and segmentation of tumor regions in Ultra Sound (US) images is important for saving the human life. At present, computer aided methods are developed for detecting the tumor regions in US images. Hence, this paper develops computer aided tumor regions detection and segmentation in ultrasound thyroid images using Hidden Markov Model (HMM). This method computes the features from both benign and malignant thyroid images from the open access database. The computed features are trained and classified into benign and malignant using the improved hidden states with HMM approach. Then, region growing algorithm is applied on the malignant image to segment the tumor pixels in the classified malignant thyroid image. This proposed tumor detection and segmentation methodology is tested on both low resolution and high resolution thyroid image dataset for evaluating the proficiency of the developed model. The performance of the proposed method is well compared with other existing methods in terms of sensitivity, specificity and tumor segmentation accuracy.**

Keywords—Thyroid; tumor; Markov; malignant; benign

I. INTRODUCTION

At present, the diseases are high in people around the world due to the improper food habits and genetic reasons. These tumors are categorized into brain tumors, lung tumors, liver tumors, breast tumors, cervical tumors and thyroid tumors [1]. Various causes and symptoms are there for every type of tumors in patients. It also depending on the age of the person, genetic behavior and working environment. In this paper, thyroid tumors are detected and segmented. Thyroid gland is an important organ in human body and this gland produces or segregates thyroid hormones. This hormone is important for balancing the other organs production life period. The parathyroid is another important type of gland which is also located the backside of the thyroid gland. This parathyroid gland is also affected if thyroid tumor is properly and timely treated. Hence, the detection of thyroid tumors in thyroid gland through ultra sound imaging is foremost important process.

Thyroid tumors are the most frequent diseases in much type of age persons in world. These tumors are formed in the thyroid nodules which is the important part of the human body to segregate the thyroid hormones. These segregated thyroid hormones [2] are used to make the other parts of the human body in healthier condition. Hence, the earlier detection of nodules in thyroid images is very important to prevent the unnecessary health problems in patients. Ultrasound scanning method is mostly preferred for the detection of the thyroid nodules or tumors, which is the most powerful screening method to screen the tumor pixels. At presently, manual work or process is required to detect the tumor pixels in the thyroid images. It is not suitable for screening the thyroid nodules in all patients having thyroid problems. Many computer aided methods are developed from the last decades to detect and segment the tumor regions in thyroid images. These methods uses complex tumor detection algorithm for locating the tumor regions.

In order to overcome such issues, soft computing methodologies is preferred for the automatic detection [3-6] and screening the tumor pixels in ultrasound thyroid images. Fig. 1 illustrates the ultrasound thyroid image.

Fig. 1. Ultrasound thyroid image.

Many conventional methods used deep learning architectures [4-6] for the detection process of thyroid tumors in ultrasound thyroid images. These methods provided different classification accuracy for different dataset images. Hence, this paper proposes a method for the efficient detection of thyroid tumors in ultrasound thyroid images using hidden Markov models.

II. Literature Survey

Reference [7] used deep learning algorithm for the screening of tumor regions in ultrasound thyroid images. This method developed various Convolutional filtering layer architectures for the detection and classifications of thyroid nodules. The authors tested this deep learning architecture based thyroid nodule detection on different dataset images. Kitahara et al. [8] discussed various thyroid nodules detection procedures for understanding the behavior of the tumor pixels in ultrasound thyroid images. The authors analyzed the time and frequency properties of the pixels in ultrasound thyroid images for the classifications of thyroid images into either benign or malignant based on the transformation of pixel domains. The authors also analyzed various set of performance metrics for the detection of thyroid tumors in the ultrasound thyroid images. Xie et al. [9] analyzed the performance of the thyroid tumor detection in frequency domain with respect to various domain dataset images. This method used modified Convolutional deep learning architecture for the classifications of each pixel in ultrasound thyroid images. The authors tested this proposed method with respect to various filter sizes and number of designed layers in order to get the high classification accuracy of the proposed thyroid nodule detection system.

Choi et al. [10] framed thyroid tumor detection system using artificial intelligence method which detected and screened the tumor pixels in ultra sound thyroid images. The authors used back propagation artificial neural networks for the detection of tumor pixels in thyroid images. The non-linear behavior of each pixel properties were analyzed with respect to its surrounding pixel properties for the efficient detection and classifications of tumor pixels. Ma et al. [11] trained the ultrasound thyroid images for the automatic detection and classifications of the source thyroid images. The authors designed their own error free back propagation based neural network architecture for the training of the proposed system. This method was tested on various types of ultrasound thyroid images in order to evaluate the performance of the proposed thyroid nodule detection system. Chi et al. [12] constructed fine-tuned deep learning Convolutional architecture for the detection of thyroid tumor pixels in ultrasound thyroid images. The authors designed this proposed system with numbers of internal layers with respect to various linear filter sizes and this method was tested on the ultrasound thyroid images in various domain databases.

III. Proposed Methodologies

This paper develops computer aided tumor regions detection in ultrasound thyroid images using Hidden Markov Model (HMM). This method computes the features from both benign and malignant thyroid images from the open access database and the computed features are classified into benign and malignant using HMM approach. Then, region growing algorithm is applied on the malignant image to segment the tumor pixels in the classified malignant thyroid image. The proposed work flow for thyroid tumor detection is illustrated in Fig. 2.

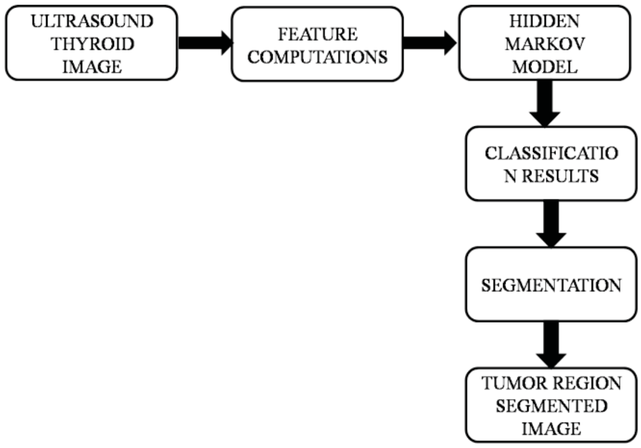

Fig. 2. Proposed ultrasound thyroid tumor detection frameworks.

A. Feature Computations

This paper computes the following features from the source ultrasound thyroid image for the classifications of benign thyroid image from the malignant thyroid image.

$$Mean = \bar{X} = \frac{\sum x_i}{N} \quad (1)$$

Where, N is the number of grey level computations in source ultrasound thyroid image.

$$Variance = \sigma^2 = \frac{\sum (x_i - \bar{X})^2}{N} \quad (2)$$

$$Skewness = \frac{1}{N} \sum_{i=1}^{N} \left| \frac{x_i - \bar{X}}{\sigma} \right|^3 \quad (3)$$

This feature is third order statistical non linear feature.

$$Kurtosis = \frac{1}{N} \sum_{i=1}^{N} \left| \frac{x_i - \bar{X}}{\sigma} \right|^4 \quad (4)$$

This feature is fourth order statistical non linear feature.

In this work, 4 features set are computed from the source single ultrasound thyroid image and this paper uses 134 ultrasound thyroid images. Hence, the total number of feature set computed from the database is 536. These computed features are given to the classifier for the classifications of normal image from the malignant thyroid image.

B. Hidden Markov Model

The classifier is the module to classify the images or objects in images into various classes using the feature set. The classifier has the classification process to differentiate the objects based on their features. Many soft computing methods are used for the past decades in order to classify the objects in to various set of sub classes. The design complexity of the developed classification methods is not suitable for the low resolution thyroid images. Hence, there is a need or requirement for developing the model to classify the tumor regions in low resolution thyroid images also.

The main novelty of this paper is to develop the model which detects and classifies the thyroid tumors in thyroid images even for low resolution mode.

In this research work, HMM approach is used for the classifications of ultrasound thyroid images into benign and malignant. This HMM approach uses probability transition matrix for calculating the nodes values for each pixels in a thyroid image.

Fig. 3 is the developed structure of the HMM for the proposed thyroid image classifications. In this proposed structure, the input nodes are defined by X1, X2 and X3. The output nodes are defined by y1, y2, y3 and y4, respectively. The input and output nodes are connected through the set of the hidden state links. These hidden state links are represented by the variable b_{ij} as illustrated in Fig. 3.

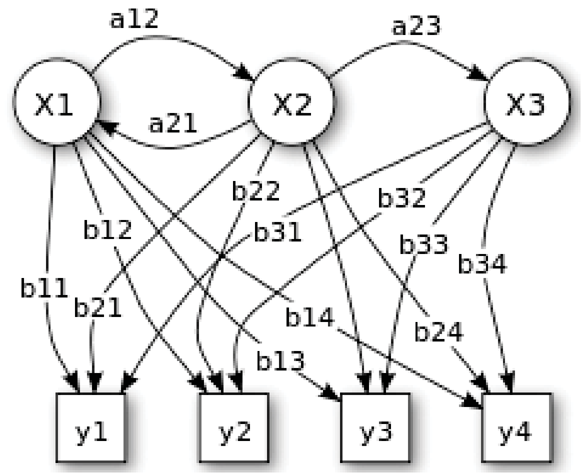

Fig. 3. Developed HMM structure.

The internal hidden state variables of the developed HMM structure is described by a single discrete random variable. The HMM model is structured with its probability transition matrix and this developed model predicts the inter hidden states for the classification of various objects in multi domain environment.

The transition probability matrix is computed using the following equation stated below.

$$H = (H_{ij}) ---\rightarrow n * n \tag{5}$$

Where, n is the number of internal nodes for each pixel in an ultrasound thyroid image and the transition probability matrix is set within the range of n.

The number of internal nodes in this proposed and developed model is depending upon the number of hidden states in the proposed design. It produces different transition probability matrix for achieving the highest classification rate of the proposed model.

This transition probability matrix is constructed with number of hidden states as described by the following mathematical equation.

$$H_{ij} = H(X_{i+1} = j | x = i) \tag{6}$$

The hidden state of the HMM approach is given by,

$$X_{i+1} \geq 0$$

This classification approach trains the ultrasound thyroid images from the open access database and also receives the source ultrasound thyroid image for the classifications of the malignant from the benign thyroid images. The features of the benign and malignant thyroid image are computed and they are trained with the developed HMM model in training stage of the proposed method. Then the features of the test or source thyroid image are computed and they are given to the pre-trained HMM model for further classification of the abnormal pixels in the test thyroid image.

After classifying the thyroid image into normal and abnormal then the tumor region segmentation process is applied on the abnormal classified thyroid images. Then, region growing algorithm is applied on the classified malignant ultrasound thyroid image for segmenting the tumor regions.

Fig. 4(a) shows the source thyroid image, Fig. 4(b) shows the tumor pixels detected and Fig. 4(c) shows the tumor region detected image.

(a) (b) (c)

Fig. 4. Tumor regions segmentation using proposed method (a) Source thyroid image (b) Tumor pixels detected (c) Tumor region detected image.

IV. Results And Discussions

This paper uses DDTI thyroid ultrasound image database [13] for analyzing the analysis of proposed tumor detection system stated in this research work. This database for ultrasound thyroid images was developed by Universidad Nacional de Colombia and they granted free access to all researchers in the field of thyroid tumor detection. This database is split into two sections as benign case and malignant case. The benign cases split-up have 33 ultrasound thyroid images and the malignant case split-up have 101 ultrasound thyroid images. All these ultrasound thyroid images are verified by two radiologists who are working in this field for the past two decades. The ultrasound thyroid images in this database are license free access for all and all the researchers do not need permission to access this dataset. The ultrasound thyroid image in this database is having the size of 256*256 pixels as image width and height, respectively.

The proposed thyroid tumor detection and segmentation system is simulated using MATLAB R2018 version in this paper. The HMM model tool box is interfaced externally with the developed model.

The features from the benign ultra sound thyroid images and malignant ultra sound thyroid images from the open access dataset are fed into the hidden state nodes of the proposed HMM structure. Then, the features from the test ultra sound thyroid image are also fed into the proposed HMM structure with the feature pattern from the pre trained HMM structure. The HMM structure in classification mode classifies the test image features into either normal or abnormal.

In this research work, the following mathematical design equations are involved to evaluate the efficiency of the proposed thyroid tumor detection system.

$$Sensitivity\,(Se)\; = \frac{P1}{P1+P4} * 100\% \tag{7}$$

$$Specificity\,(Sp)\; = \frac{P2}{P2+P4} * 100\% \tag{8}$$

$$TumorSegmentationAccuracy\,(TSA) = \frac{P1+P2}{P1+P2+P3+P4} * 100\% \tag{9}$$

$$PositiveLikelihoodMetric\,(PLM) = \frac{Se}{1-Sp} * 100\% \tag{10}$$

$$NeagtiveLikelihoodMetric\,(NLM) = \frac{1-Se}{Sp} * 100\% \tag{11}$$

The sensitivity and specificity is the representations of the number of tumor pixels correctly classified with respect to ground truth images in this paper. The segmented tumors efficiency is defined by the tumor segmentation accuracy. The PLM and NLM are defined by the impact of the non-tumor pixels detection in the proposed method.

The proposed ultrasound thyroid tumor detection framework stated in this work is independently tested on the two modes of ultrasound thyroid images as low resolution and high resolution image cases. Most of the conventional thyroid tumor detection methods provided good simulation results for high resolution ultrasound thyroid images only [14-16] and provided low performance efficiency for low resolution ultrasound thyroid images. Hence, the proposed methods stated in this research work are checked on both resolution image dataset.

Table I shows the analysis of proposed thyroid tumor segmentation on low resolution images in terms of sensitivity, specificity, tumor segmentation accuracy, Positive likelihood metric and negative likelihood metric, respectively.

TABLE I. ANALYSIS OF PROPOSED THYROID TUMOR SEGMENTATION ON LOW RESOLUTION IMAGES

Ultrasound thyroid image sequences	Performance metrics for the proposed work				
	Se	***Sp***	***TSA***	***PLM***	***NLM***
1	95.7	98.1	98.9	96.7	98.9
2	96.1	98.6	99.1	97.1	98.1
3	97.5	98.5	99.6	98.4	98.6
4	97.1	98.9	99.6	96.9	97.9
5	98.6	98.4	99.8	98.4	98.3
6	90.7	98.6	99.4	96.7	98.6
7	96.9	98.1	98.6	98.1	97.9
8	97.8	98.4	98.3	96.9	98.5
9	98.1	98.3	98.8	97.4	98.7
10	98.9	98.2	98.9	98.1	98.5
Average	**96.74**	**98.41**	**99.1**	**97.47**	**98.4**

The proposed ultrasound thyroid tumor detection method in this work achieves 96.74% of Se, 98.41% of Sp, 99.1% of TSA, 97.47% of PLM and 98.4% of NLM, on low resolution thyroid images. Fig. 5 shows the graphical analysis of proposed thyroid tumor segmentation on low resolution images.

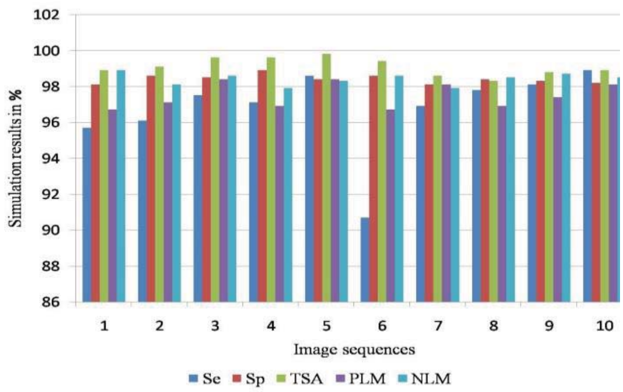

Fig. 5. Graphical analysis of proposed thyroid tumor segmentation on low resolution images.

Table II shows the analysis of proposed thyroid tumor segmentation on high resolution images in terms of sensitivity, specificity, tumor segmentation accuracy, Positive likelihood metric and negative likelihood metric, respectively. The proposed ultrasound thyroid tumor detection method in this work achieves 98.32% of Se, 98.82% of Sp, 99.34% of TSA, 99% of PLM and 98.97% of NLM, on high resolution thyroid images.

TABLE II. ANALYSIS OF PROPOSED THYROID TUMOR SEGMENTATION ON HIGH RESOLUTION IMAGES

Ultrasound thyroid image sequences	Performance metrics for the proposed work				
	Se	*Sp*	*TSA*	*PLM*	*NLM*
1	97.8	98.9	99.9	98.7	98.9
2	98.7	98.9	99.1	98.6	99.1
3	98.9	98.5	99.6	98.4	98.6
4	98.6	98.9	99.6	98.9	99.6
5	98.4	99.4	99.8	98.4	98.3
6	99.1	98.6	99.4	99.7	98.6
7	96.9	99.1	99.5	99.8	98.9
8	97.8	98.4	98.3	99.7	99.5
9	98.1	99.3	99.3	99.7	98.7
10	98.9	98.2	98.9	98.1	99.5
Average	**98.32**	**98.82**	**99.34**	**99**	**98.97**

Fig. 6 shows the graphical analysis of proposed thyroid tumor segmentation on high resolution images.

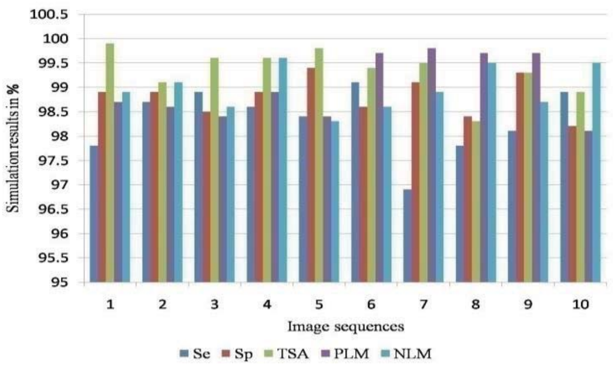

Fig. 6. Graphical analysis of proposed thyroid tumor segmentation on high resolution images.

Table III shows the comparisons of proposed thyroid tumor segmentation work on different image resolution datasets.

TABLE III. COMPARISONS OF THE PROPOSED METHOD ON LOW AND HIGH RESOLUTION DATASET

Performance metrics	DDTI thyroid ultrasound image database	
	Low resolution dataset	*High resolution dataset*
Se	96.74	98.32
Sp	98.41	98.82
TSA	99.1	99.34
PLM	97.47	99
NLM	98.4	98.97

Fig. 7 shows the graphical comparisons of proposed thyroid tumor segmentation work on different image resolution datasets.

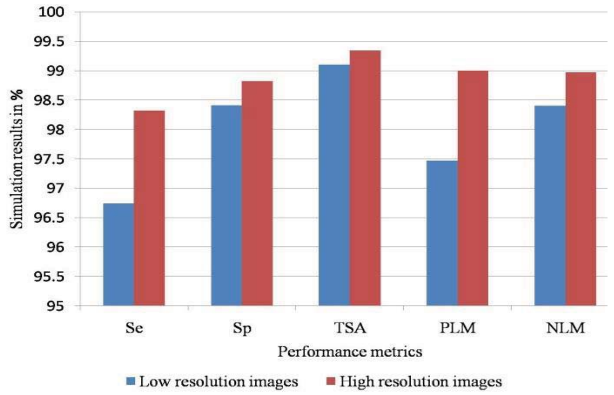

Fig. 7. Graphical comparisons of proposed thyroid tumor segmentation work on different image resolution datasets.

Table IV shows the comparisons of proposed thyroid tumor segmentation work on other methods.

TABLE IV. PERFORMANCE COMPARISONS

Performance metrics	Performance metrics		
	Se(%)	*Sp(%)*	*Acc(%)*
Proposed work	98.32	98.82	99.34
Chai et al. [7]	96.7	97.19	98.18
Xie et al. [9]	98.12	97.26	97.99

V. CONCLUSIONS

The analysis of proposed thyroid tumor segmentation stated in this paper is tested on low resolution images in terms of sensitivity, specificity, tumor segmentation accuracy, Positive likelihood metric and negative likelihood metric, respectively. The proposed ultrasound thyroid tumor detection method in this work achieves 96.74% of Se, 98.41% of Sp, 99.1% of TSA, 97.47% of PLM and 98.4% of NLM, on low resolution thyroid images. The proposed ultrasound thyroid tumor detection method in this work achieves 98.32% of Se, 98.82% of Sp, 99.34% of TSA, 99% of PLM and 98.97% of NLM, on high resolution thyroid images. The simple algorithm of the proposed work is the main advantage of this paper for thyroid tumor detection and segmentation. The main limitation of this proposed method is that this requires large number of low and high resolution ultra sound thyroid images for both training and testing. The future work extension of this paper is to implement the deep learning algorithm for the detection of tumors regions in thyroid images.

ACKNOWLEDGMENT

The images used in this paper are attained from open access dataset http://wilmingtonendo.com/image-gallery/

REFERENCES

[1] R.A. DeLellis, R.V. Lloyd, P.U. Heitz, C. Eng, "World Health Organization Classification of Tumours," Pathology and Genetics of Tumours of Endocrine Organs, IARC Press, Lyon, France, 2004.

[2] C. Cappelli, M. Braga, E. De Martino, et al., "Outcome of patients surgically treated for various forms of hyperthyroidism with differentiated thyroid cancer: experience at an endocrine center in Italy," Surgery Today, vol. 36, no. 2, pp. 125-130, 2006.

[3] L. Wang, S. Yang, S. Yang, et al., "Automatic thyroid nodule recognition and diagnosis in ultrasound imaging with the YOLOv2 neural network," World J Surg Onc., vol. 17, no. 12, 2019.

[4] Kaiming He, Xiangyu Zhang, Shaoqing Ren, Jian Sun, "Deep residual learning for imaging recognition," IEEE Conf Comput Vision Pattern Recognit., vol. 2016, pp. 770-778, 2016.

[5] K. Nakamura, H. Yoshida, R. Engelmann, H. MacMahon, S. Katsuragawa, T. Ishida, et al., "Computerized analysis of the likelihood of malignancy in solitary pulmonary nodules with use of artificial neural networks," Radiology, vol. 214, pp. 823-830, 2000.

[6] L. Cantalamessa, M. Baldini, A. Orsatti, L. Meroni, V. Amodei, D. Castagnone, "Thyroid nodules in Graves disease and the risk of thyroid carcinoma," JAMA Internal Medicine, vol. 159, no. 15, pp. 1705-1708, 1999.

[7] Y.J. Chai, J. Song, Mohammad Shaear, K.H. Yi, "Artificial intelligence for thyroid nodule ultrasound image analysis", Annals of Thyroid, vol. 5, no. 8, pp. 1-5, 2020.

[8] C.M. Kitahara, J.A. Sosa, "Understanding the ever-changing incidence of thyroid cancer," Nat Rev Endocrinol, vol. 16, pp. 617-618, 2020.

[9] S. Xie, J. Yu, T. Liu, Q. Chang, L. Niu and W. Sun, "Thyroid Nodule Detection in Ultrasound Images with Convolutional Neural Networks," 14th IEEE Conference on Industrial Electronics and Applications (ICIEA), Xi'an, China, pp. 1442-1446, 2019.

[10] Y.J. Choi, J.H. Baek, H.S. Park, et al. "A Computer-Aided Diagnosis System Using Artificial Intelligence for the Diagnosis and Characterization of Thyroid Nodules on Ultrasound: Initial Clinical Assessment," Thyroid, vol. 27, pp. 546-552, 2017.

[11] J. Ma, F. Wu, J. Zhu, D. Xu and D. Kong, "A pre-trained convolutional neural network based method for thyroid nodule diagnosis," Ultrasonics, vol. 73, pp. 221-230, 2017.

[12] J. Chi, E. Walia, P. Babyn, J. Wang, G. Groot and M. Eramian, "Thyroid nodule classification in ultrasound images by fine-tuning deep convolutional neural network," Journal of Digital Imaging, vol. 30, no. 4, pp. 477-486, 2017.

[13] DDTI thyroid ultrasound image database, Available at: <http://cimalab.intec.co/?lang=en&mod=project&id=31>.

[14] Akselrod-Ballin, L. Karlinsky, S. Alpert, S. Hasoul, R. Ben-Ari and E. Barkan, "A region based convolutional network for tumor detection and classification in breast mammography," Deep Learning and Data Labeling for Medical Applications, Springer, pp. 197-205, 2016.

[15] P.F. Felzenszwalb, R.B. Girshick, D. McAllester and D. Ramanan, "Object detection with discriminatively trained part-based models," IEEE Transactions on Pattern Analysis and Machine Intelligence, vol. 32, no. 9, pp. 1627-1645, 2010.

[16] J. Redmon, S. Divvala, R. Girshick and A. Farhadi, "You only look once: Unified real-time object detection," Proceedings of the IEEE conference on computer vision and pattern recognition, pp. 779-788, 2016.